Earth and Planetary Science Letters 400 (2014) 261–271

Contents lists available at ScienceDirect

Earth and Planetary Science Letters

www.elsevier.com/locate/epsl

Assessing orbitally-forced interglacial climate variability during the mid-Pliocene Warm Period

Caroline L. Prescott *, Alan M. Haywood, Aisling M. Dolan, Stephen J. Hunter, James O. Pope, Steven J. Pickering

School of Earth and Environment, Earth and Environment Building, University of Leeds, Woodhouse Lane, Leeds, LS2 9JT, UK

ARTICLE INFO

Article history:
Received 21 February 2014
Received in revised form 8 May 2014
Accepted 19 May 2014
Available online 12 June 2014
Editor: J. Lynch-Stieglitz

Keywords:
palaeoclimate
Pliocene
climate model
variability
KM5c
K1

ABSTRACT

The traditional view of the Pliocene is one of an epoch with higher than present global mean annual temperatures (~2 to 3 °C) and stable climate conditions. Published data-model comparisons for the mid-Pliocene Warm Period (mPWP: ~3.3 to 3 million years ago) have identified specific regions of concordance and discord between climate model outputs and marine/terrestrial proxy data. Due to the time averaged nature of global palaeoenvironmental syntheses, it has been hypothesised that climate variability during interglacial events within the mPWP could contribute to site-specific data/model disagreement. The Hadley Centre Coupled Climate Model Version 3 (HadCM3) is used to assess the nature of climate variability around two interglacial events within the mPWP that have different characteristics of orbital forcing (Marine Isotope Stages KM5c and K1). Model results indicate that ±20 kyr on either side of the MIS KM5c, orbital forcing produced a less than 1 °C change in global mean annual temperatures. Regionally, mean annual surface air temperature (SAT) variability can reach 2 to 3 °C. Seasonal variations exceed those predicted for the annual mean and can locally exceed 5 °C. Simulations 20 kyr on either side of MIS K1 show considerably increased variability in relation to KM5c.

We demonstrate that orbitally-forced changes in surface air temperature during interglacial events within the mPWP can be substantial, and could therefore contribute to data/model discord. This is especially likely if proxies preserve growing season rather than mean annual temperatures.

Model results indicate that peak MIS KM5c and K1 interglacial temperatures were not globally synchronous, highlighting leads and lags in temperature in different regions. This highlights the potential pitfalls in aligning peaks in proxy-derived temperatures across geographically diverse data sites, and indicates that a single climate model simulation for an interglacial event is inadequate to capture peak temperature change in all regions.

We conclude that the premise of sustained global warmth and stable Pliocene climate conditions is incomplete. We also contend that the likely nature of Pliocene interglacial climate variability is more akin to interglacial events within the Quaternary, where the character of interglacials is known to be diverse. In the future, the utility of Pliocene data/model comparisons is dependent upon 1) establishing precise chronology of the proxy data, 2) providing climate models with fully proxy-consistent boundary conditions and 3) in utilising ensembles of climate simulations that can adequately capture orbital variability around any studied interval.

1. Introduction

1.1. Modelling Pliocene climate

Geological data, as well as climate model outputs, have shed considerable light on the nature of Pliocene climate and environments. During Pliocene warmth, highlighted by negative excursions in $\delta^{18}O$ from benthic foraminifera, Antarctic and/or Greenland ice volume may have been reduced (Shackleton and Hall, 1984; Lunt et al., 2008; Naish et al., 2009; Pollard and DeConto, 2009; Hill et al., 2010; Dolan et al., 2011). Peak sea-level high stands have been estimated to have been 22 ± 5 m higher than modern (Miller et al., 2012). Sea surface temperatures (SSTs) were warmer (Dowsett et al., 2010), particularly in the higher latitudes and upwelling zones (e.g. Dekens et al., 2007; Dowsett et

* Corresponding author. Tel.: +44113 3439085.
E-mail address: js07c2lp@leeds.ac.uk (C.L. Prescott).

http://dx.doi.org/10.1016/j.epsl.2014.05.030
0012-821X/

al., 2012; Rosell-Melé et al., 2014). Sea-ice cover also declined substantially (e.g. Cronin et al., 1993; Polyak et al., 2010; Moran et al., 2006). On land, the global extent of arid deserts decreased, and forests replaced tundra in the Northern Hemisphere (e.g. Salzmann et al., 2008). The global mean annual temperature may have increased by 2 to 3 °C (e.g. Haywood and Valdes, 2004; Haywood et al., 2013a). Meridional and zonal temperature gradients may have been reduced, which had a significant impact on the Hadley and Walker circulation (e.g. Haywood et al., 2000; Chan et al., 2011). The East Asian Summer Monsoon, as well as other monsoon systems, may have been enhanced (e.g. Wan et al., 2010).

Arguably the best geologically studied interval of the Pliocene is the mid-Pliocene warm period (mPWP) between 3264 and 3025 ka (Dowsett et al., 2010; Haywood et al., 2010). It sits within the Piacenzian age of the Late Pliocene according to the geological timescale of Gradstein et al. (2004). The mPWP has been the focus of a number of modelling efforts that have employed individual snap-shot style climate simulations to explore the nature of global climate at this time, as well as the sensitivity of simulated global and regional climates to imposed Pliocene boundary conditions (e.g. Haywood et al., 2013a). The mPWP has also been a focus for a specific targeted campaign of data collection as well as modelling, under the PRISM (Pliocene Research Interpretations and Synoptic Mapping) approach.

1.2. Data/model comparison and climate variability

Given the abundance of proxy data, the mPWP has become a focus for data/model comparisons that attempt to analyse the ability of climate models to reproduce a warm climate state in Earth history (e.g. Haywood and Valdes, 2004; Salzmann et al., 2008; Dowsett et al., 2011, 2012; Haywood et al., 2013a; Salzmann et al., 2013). Whilst these studies have shown areas of agreement between climate model outputs and geological proxy temperature estimates, discord has been noted in the North Atlantic, as well as the high-latitudes in general. In these areas climate models underestimate the degree of polar amplification recorded in proxy data (Dowsett et al., 2012; Salzmann et al., 2013). If true these results are potentially of great importance in understanding the sensitivity of models for simulating warm climate states.

In any palaeo-data/model comparison the cause of data/model discord will be complex and not easily attributable to a single factor in either the models or proxy data. One aspect that requires consideration is the proxy data that provide surface temperature estimates which are compared with climate model outputs. In the Pliocene, and in deep time in general (pre-Quaternary), some of the most important uncertainty in proxy data used for data model comparison can be attributed to chronology, correlation and the time averaged nature of existing global palaeoenvironmental syntheses. This is in addition to inherent uncertainties with proxies stemming from non-modern analogue environments, evolutionary changes of ecological tolerance and methodological problems. In the context of the Pliocene, limitations in correlating one marine or land site to another over large geographical distances originally favoured the establishment of a time slab to which the ages of marine or terrestrial sites could be more confidently attributed (Dowsett and Poore, 1991). The time slab for the PRISM3D (Pliocene Research, Interpretation and Synoptic Mapping) global marine synthesis was ~240 kyr long (Dowsett et al., 2010). The global vegetation reconstruction within PRISM3D was constructed by considering information from the entire Piacenzian Stage of the Pliocene epoch, ~1000 kyr in duration (Salzmann et al., 2008).

The PRISM mPWP global environmental syntheses represent an average of warm climate signals from site to site for a defined time slab (Dowsett et al., 2010; Salzmann et al., 2008). They should not be considered as reconstructions of environmental conditions that existed together at a discrete moment in time. Climate model simulations are run for short integration periods (i.e. several centuries) using a single realisation of orbital, CO_2 and other forcings, and are not able to reproduce syntheses of average warm climate conditions (e.g. spanning ~240 to 1000 kyr), which must by definition reflect multiple changing and interacting forcing mechanisms (i.e. show climate variability). Haywood et al. (2013b) hypothesise that a component of currently noted model/data inconsistencies are related to the time slab nature of the global environmental syntheses and the limited characterisation of Pliocene climate variability in existing proxy data and climate model simulations.

Here we explore this hypothesis by completing a series of orbital forcing sensitivity experiments using the Hadley Centre Coupled Climate Model version 3 (HadCM3) around two discrete interglacial events within the mPWP (Marine Isotope Stages KM5c (3205 ka) and K1 (3060 ka); Fig. 1). For the purposes of this paper we define a Pliocene interglacial as any isotope excursion which results in more negative $\delta^{18}O$ than the Holocene average. Whilst the nature of discrete boundary conditions (e.g. the ice sheet configuration) for individual interglacial events within the mPWP remains unknown, we are able to quantify the magnitude of orbitally-forced climate variability in each interglacial event, and how the variability in each interglacial differs. Haywood et al. (2013b) show that the peak of Marine Isotope Stage (MIS) KM5c is characterised by a near modern orbital forcing within a period of low eccentricity and low precession. In contrast MIS K1 occurred during an interval where the total global mean annual insolation was ~0.5 $W\,m^{-2}$ higher than the modern. It is characterised by one of the lightest benthic oxygen isotope excursions evident in the mPWP.

2. Methodology

2.1. Model description – HadCM3

The particulars of the UK Met Office Hadley Centre Coupled Climate Model Version 3 (HadCM3) used in this study are well documented (Gordon et al., 2000). The model requires no flux corrections, even for simulations of a thousand years or more (Gregory and Mitchell, 1997). HadCM3 consists of a coupled atmosphere, ocean and sea ice model components. The horizontal resolution of the atmospheric model is 2.5° in latitude by 3.75° in longitude. This gives a grid spacing at the equator of 278 km in the north–south direction and 417 km east–west and is approximately comparable to a T42 spectral model resolution. The atmospheric model consists of 19 layers. The atmospheric model has a time step of 30 min and includes a radiation scheme that can represent the effects of minor trace gases (Edwards and Slingo, 1996). A parameterisation of simple background aerosol climatology is also included (Cusack et al., 1998). The convection scheme is described in Gregory et al. (1997). A land-surface scheme includes the representation of the freezing and melting of soil moisture. The representation of evaporation includes the dependence of stomatal resistance on temperature, vapour pressure and CO_2 concentration (Cox et al., 1999).

The spatial resolution of the ocean is 1.25 by 1.25°. The model has 20 layers and includes the use of the Gent–McWilliams mixing scheme (Gent and McWilliams, 1990). The sea ice model uses a simple thermodynamic scheme and contains parameterisations of ice drift and leads (Cattle and Crossley, 1995).

2.2. Boundary conditions and experimental design

Essential boundary conditions for our Pliocene simulations are based on, or modified from, those used within the Pliocene Model

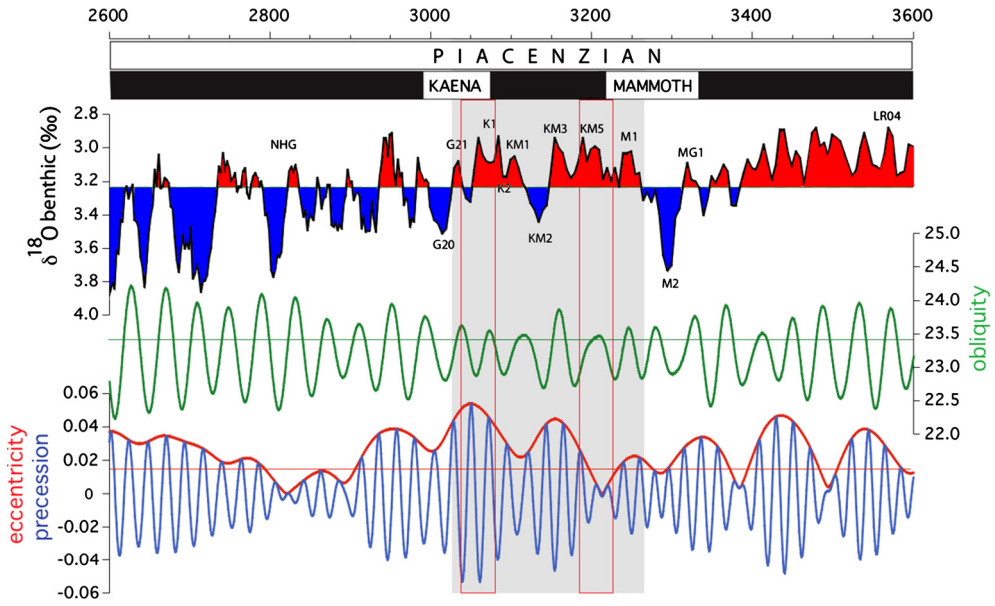

Fig. 1. Position of the K1 and KM5c interglacials and the PRISM3D time slab (grey shaded band) on the Lisiecki and Raymo (2005) benthic oxygen isotope stratigraphy horizontal line showing the Holocene average. Obliquity, precession and eccentricity as derived from the astronomical solution of Laskar et al. (2004; La04) are also shown with the horizontal lines showing the modern orbital values.

Intercomparison Project (PlioMIP) coupled atmosphere–ocean simulation, which is described in detail in Haywood et al. (2011). In brief this PlioMIP simulation uses the US Geological Survey PRISM3D boundary condition data set (Dowsett et al., 2010; http://geology.er.usgs.gov/eespteam/prism/prism_pliomip_data.html), and the PlioMIP submission for HadCM3 is presented in Bragg et al. (2012).

In PlioMIP a modern orbital configuration is specified and atmospheric trace gasses are set to pre-industrial levels, except CO_2 which is specified at 405 ppmv. All simulations were integrated for 500 years (unless otherwise stated), with the final 100 years used to calculate the required climatological means. Table 1 provides summary details of all HadCM3 experiments included in this study. Time series analyses show no significant globally integrated trends in surface climate for the averaging period, indicating that the surface climatology of the model has reached an equilibrium state.

2.3. KM5c and K1 orbital forcing sensitivity experiments

Initially we have performed two control simulations for the KM5c ($Plio^{CTL}KM5c^{3205}$) and K1 ($Plio^{CTL}K1^{3060}$) interglacials. Using orbital parameters derived from the astronomical solution of Laskar et al. (2004), we have modified HadCM3 to be representative of orbital forcing at the interglacial events, 3205 and 3060 ka. Due to precessional effects amplified by changes in eccentricity, the length of seasons evolves through time (Joussaume and Braconnot, 1997). This "calendar effect" has no impact on the mean annual SATs but has potential to introduce inaccuracy/bias to the interpretation of seasonal SATs. In this study, we have assessed that the seasonal results shown are not sensitive to this "calendar effect".

Additionally, we have carried out a suite of 30 orbital sensitivity simulations that are centred on the two selected isotope excursions. For 20 kyr preceding and postdating KM5c a total of 20 simulations were carried out (a simulation every 2 kyr). The 20 kyr window was selected in order to best capture a plausible scenario of uncertainty in chronological control for new proxy records produced. Using the experience gained from the KM5c sensitivity experiments, we were able to determine that a 4 kyr spacing between experiments was sufficient to capture the nature of orbitally forced SAT variability. Therefore, we have only performed experiments every 4 kyr around K1 (see Table 1). These sensitivity experiments enable us to quantify the orbital forcing contribution to climate change for two intervals of time spanning 40 kyr each. For convenience we have adopted the notation $Plio\_KM5c^{Year}$ to describe each KM5c sensitivity experiment. For example $Plio\_KM5c^{3203}$ represents the orbital sensitivity experiment 2 kyr after the peak of the KM5c interglacial event (see Table 1). We have also followed a similar notation system for the K1 sensitivity experiments, whereby $Plio\_K1^{3056}$ denotes the simulations 2 kyr after the K1 peak.

3. Results

3.1. Magnitude of orbitally forced changes in SAT (KM5c 3185 to 3225 ka)

Fig. 2 shows the difference in mean annual SAT between the KM5c/K1 control simulations and the standard pre-industrial control simulation (see also Haywood et al., 2013b). Fig. 3 displays global mean annual SAT anomalies (compared to $Plio^{CTL}KM5c^{3205}$) predicted by HadCM3 for 10 of the orbital sensitivity simulations. During the 40 kyr interval sampled around KM5c, the global annual mean temperature ranges from 18.04 °C ($Plio^{CTL}KM5c^{3205}$) to 18.25 °C ($Plio\_KM5c^{3197, 3193 \text{ and } 3191}$), see Table 1. The most striking observation from the results displayed in Fig. 3 are the vast areas of the Earth's surface that do not show any statistical significant differences from the KM5c control experiment. In general, experiments representative of the time window prior to the KM5c interglacial peak (i.e. $Plio\_KM5c^{3225}$ to $Plio\_KM5c^{3209}$) are cooler than peak itself. Those after KM5c (i.e. $Plio\_KM5c^{3201}$ to $Plio\_KM5c^{3185}$) are warmer (Fig. 3). The spatial patterns exhibited in the temperature anomalies can be broadly categorised into three groups; (i) nominal differences, (ii) experiments which display a dipole feature of temperature change in the North Atlantic, and (iii) experiments which display terrestrial surface temperature changes of greater than 1 °C.

Experiments exhibiting nominal, or statistically insignificant (when assessed by a Student's t-test at the 95% confidence interval), deviation from $Plio^{CTL}KM5c^{3205}$ include, $Plio\_KM5c^{3217}$,

Table 1
Summary of experiments including orbital parameters implemented in HadCM3 and global mean annual and seasonal temperatures. Controls indicated in bold.

Experiment name	Eccentricity	Precession	Obliquity	MAT (°C)	JJA (°C)	DJF (°C)
Plio_KM5c^{3225}	0.01	−0.003998	22.92704	18.05	20.11	15.92
Plio_KM5c^{3223}	0.01	0.001968	23.01538	18.04	20.00	15.99
Plio_KM5c^{3221}	0.01	0.005338	23.12036	18.10	19.99	16.12
Plio_KM5c^{3219}	0.01	0.005455	23.22784	18.05	19.98	16.02
Plio_KM5c^{3217}	0.00	0.003253	23.32529	18.06	20.05	15.98
Plio_KM5c^{3215}	0.00	0.000577	23.40339	18.07	20.13	15.91
Plio_KM5c^{3213}	0.00	−0.000684	23.45685	18.13	20.20	15.99
Plio_KM5c^{3211}	0.00	0.000348	23.48581	18.07	20.11	15.96
Plio_KM5c^{3209}	0.00	0.003001	23.49423	18.14	20.11	16.09
Plio_KM5c^{3207}	0.01	0.005561	23.48812	18.09	20.02	16.06
Plio^{CTL}KM5c^{3205}	0.01	0.006048	23.47363	18.04	20.00	15.98
Plio_KM5c^{3203}	0.01	0.003145	23.45559	18.08	20.11	15.94
Plio_KM5c^{3201}	0.01	−0.002863	23.43613	18.14	20.34	15.86
PlioKM5c^{3199}	0.01	−0.009965	23.41459	18.16	20.48	15.78
Plio_KM5c^{3197}	0.02	−0.015177	23.38809	18.20	20.59	15.78
Plio_KM5c^{3195}	0.02	−0.015627	23.35229	18.22	20.57	15.84
Plio_KM5c^{3193}	0.02	−0.009880	23.30298	18.24	20.39	16.05
Plio_KM5c^{3191}	0.02	0.001086	23.23714	18.21	20.09	16.26
Plio_KM5c^{3189}	0.02	0.013936	23.15446	18.16	19.78	16.44
Plio_KM5c^{3187}	0.03	0.023878	23.05862	18.12	19.59	16.50
Plio_KM5c^{3185}	0.03	0.026414	22.95756	18.11	19.64	16.43
Plio_K1^{3080}	0.04	−0.024808	23.31512	18.50	20.91	16.11
Plio_K1^{3076}	0.04	0.019597	23.51012	18.51	19.86	17.05
Plio_K1^{3072}	0.05	0.046580	23.57159	18.41	19.48	17.18
Plio_K1^{3068}	0.05	0.021245	23.46148	18.60	20.49	16.49
Plio_K1^{3064}	0.05	−0.032116	23.23327	18.71	21.65	15.75
Plio^{CTL}K1^{3060}	0.05	−0.050860	23.00698	18.79	21.89	15.87
Plio_K1^{3056}	0.05	−0.008461	22.90429	18.76	20.58	16.88
Plio_K1^{3052}	0.05	0.045905	22.98374	18.58	19.43	17.61
Plio_K1^{3048}	0.05	0.045280	23.20710	18.60	19.92	17.07
Plio_K1^{3044}	0.05	−0.009171	23.46148	18.76	21.31	16.06
Plio_K1^{3040}	0.05	−0.050801	23.62471	18.88	22.13	15.73

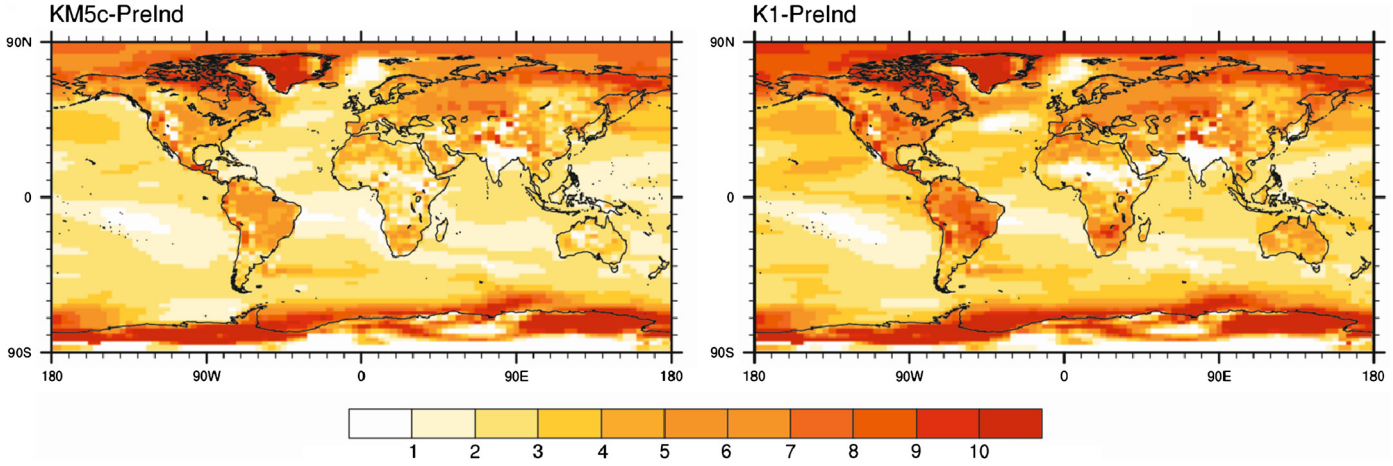

Fig. 2. Annual mean Pliocene SAT predictions from HadCM3: (left) interglacial MIS KM5c minus a pre-industrial experiment; (right) interglacial MIS K1 minus a pre-industrial experiment.

Plio_KM5c^{3213}, Plio_KM5c^{3209}. One of the major features predicted by HadCM3 to varying degrees is a dipole in temperature change in the North Atlantic. This feature of cooling, which begins at the coast of Newfoundland and propagates Eastward across the Atlantic, coupled with a warming centred off the Southern tip of Greenland and into the Labrador Sea is apparent in eight of the twenty KM5c sensitivity simulations. Often this pattern of temperature change is also associated with a large temperature anomaly around Svalbard (e.g. Plio_KM5c^{3215}). The temperature dipole is strongest (>2 °C) in experiments Plio_KM5c^{3201} and Plio_KM5c^{3189}. Simulations conducted for the time period between Plio_KM5c^{3197} and Plio_KM5c^{3185} all demonstrate a significant terrestrial warming over parts of South America, South Africa and India of up to 2 °C. Please refer to Supplementary Fig. 2 for the further 10 KM5c orbital sensitivity anomaly plots.

Some experiments do not easily fall into one of the categories identified above. In Plio_KM5c^{3225} significant changes (up to 2 °C cooling) are limited to the high latitudes including Antarctica, sea ice marginal regions and the North Atlantic. Plio_KM5c^{3221} displays a cooling over the interior of Antarctica and a moderate (less than −1 °C) warming around Svalbard. Finally, Plio_KM5c^{3197} displays isolated regions of warming, for example over Svalbard and the wider Arctic sea ice region, in North America and around the Antarctic margins.

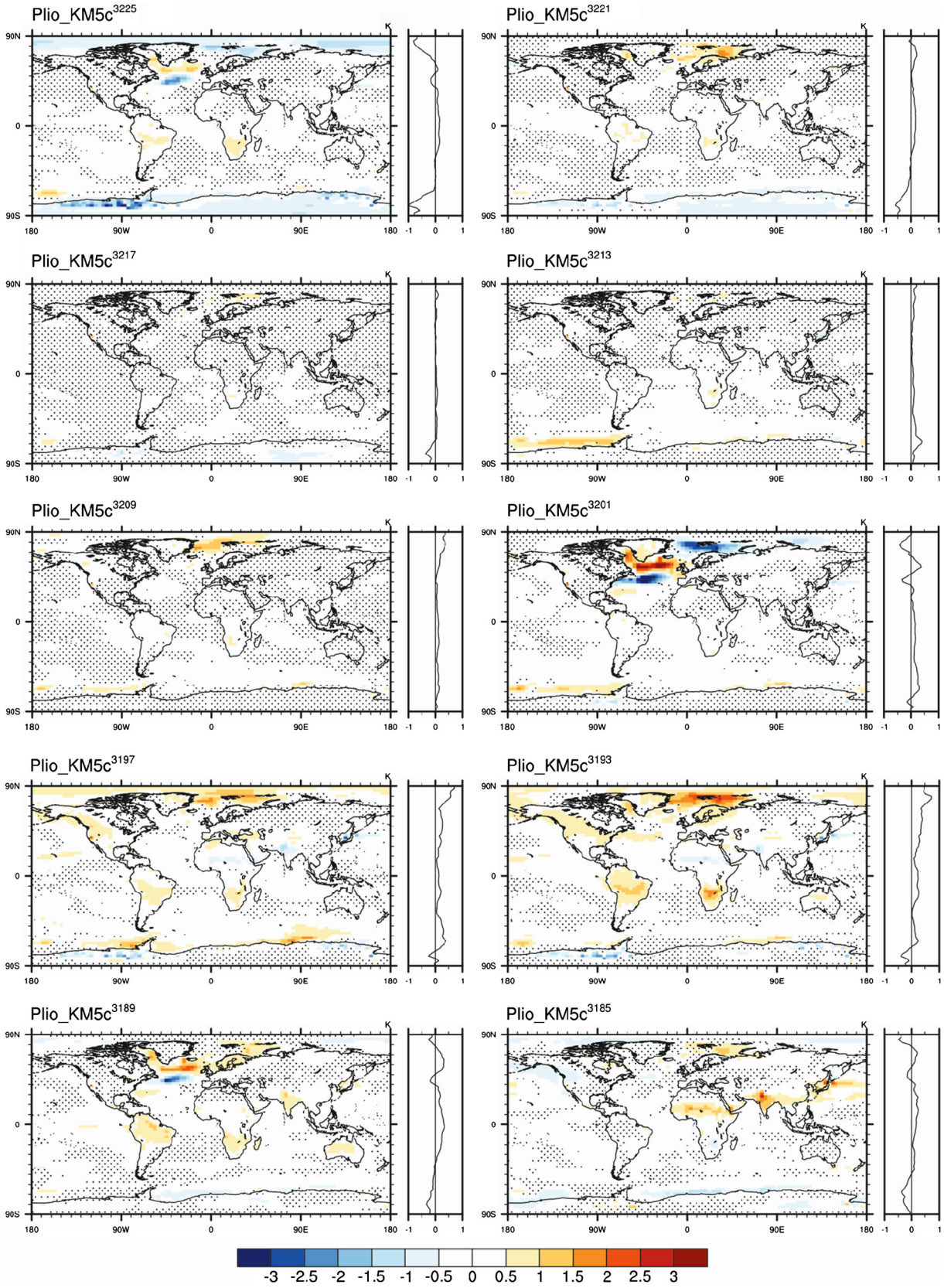

Fig. 3. Annual mean Pliocene SAT (°C) predictions from HadCM3 for 10 orbital sensitivity simulations minus the MIS KM5c control ($Plio^{CTL}KM5c^{3205}$). Stippling indicates the SAT changes that are statistically insignificant according to the Student's t-test. Zonal SAT anomalies are shown to the right of each simulation.

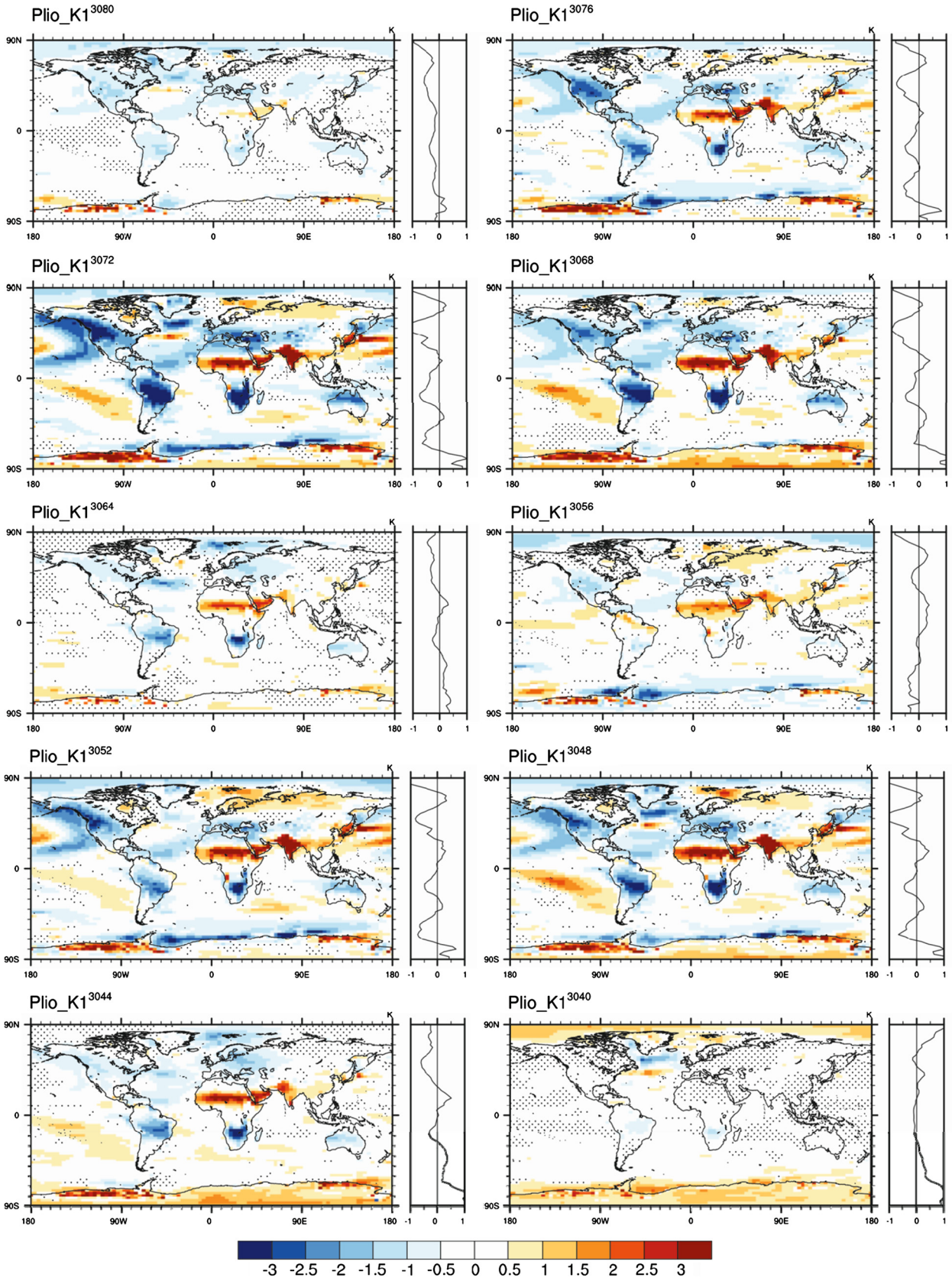

Fig. 4. Annual mean Pliocene SAT (°C) predictions from HadCM3 for 10 orbital sensitivity simulations minus the MIS K1 control ($Plio^{CTL}K1^{3060}$). Stippling indicates the SAT changes that are statistically insignificant according to the Student's t-test. Zonal SAT anomalies are shown to the right of each simulation.

3.2. Magnitude of orbitally forced changes in SAT (K1 3040 to 3080 ka)

Fig. 4 shows the global SAT anomalies from Plio^{CTL}K1^{3060} for 10 orbital sensitivity experiments with HadCM3. The global mean annual temperature ranges from 18.4 °C (Plio_K1^{3072}) to 18.85 °C (Plio_K1^{3040}). The spatial patterns shown in Fig. 4 can be approximately grouped as (i) patterns of warming and cooling exceeding 2 °C and (ii) patterns of warming and cooling not exceeding 2 °C.

Experiments showing the strongest SAT anomalies were Plio_K1^{3048}, Plio_K1^{3052}, Plio_K1^{3068} and Plio_K1^{3072} with most differences demonstrated to be statistically significant. There is cooling at the high northern latitudes (−1.5 °C) with areas of terrestrial cooling over North and South America, Southern Africa, Europe, Greenland and Australia, with some temperature anomalies (such as over South America and Southern Africa) reaching 4 °C. Equatorial terrestrial regions such as India and Central Africa exhibit a warming of up to 4 °C and 3 °C over Antarctica. Simulations Plio_K1^{3044}, Plio_K1^{3056}, Plio_K1^{3064} and Plio_K1^{3076} show a very similar pattern of temperature change to the previously discussed simulations, but with most temperature variations not exceeding ±2 °C and larger areas showing statistically insignificant temperature changes. Plio_K1^{3044} and Plio_K1^{3064} predict warming in the Svalbard area of up to 2 °C, whereas Plio_K1^{3056} and Plio_K1^{3076} show cooling in this area of up to 2 °C. Plio_K1^{3076} displays high latitude warming in the southern hemisphere of up to 4 °C. The simulations Plio_K1^{3040} and Plio_K1^{3080} show the least amount of temperature change in Fig. 4. Plio_K1^{3040} predicts predominantly cooling of up to 1.5 °C and Plio_K1^{3080}, warming in the high latitudes of up to 2 °C.

3.3. Patterns of maximum spatial variation in SAT

In order to determine the maximum difference in SAT within the two ensembles (KM5c and K1) we have examined all of the sensitivity experiments, and for each grid box selected the experiment that displays the maximum deviation from the associated control simulation (i.e. Plio^{CTL}KM5c^{3205} and Plio^{CTL}K1^{3060}). Using this information we have constructed a composite figure (Fig. 5) that demonstrates the spatial variation in maximum SAT difference.

There is a maximum orbitally induced variation in SATs of less than 1 °C around KM5c. An exception is the North Atlantic, Labrador Sea and Arctic Ocean where HadCM3 predicts differences of up to 4.8 °C. This is associated with the experiments that displayed the dipole in North Atlantic SATs discussed in Section 3.1. The variation in these regions is linked to changes in the geographical location of deep water formation, which itself is associated with a seasonal redistribution in sea ice cover, brine rejection and salinity.

To examine the dipole feature further simulations showing high variation in these regions were continued for an additional 500 simulated years. Following a greater integration length the amount of variation displayed in these regions declined. For example, differences in SAT are reduced from a maximum of 5 °C in the North Atlantic to 2 °C in the same grid squares. Thus, the higher variation predicted in these regions, compared to other regions, could simply be an artefact of model spin up. However, this is difficult to conclude with certainty. Given the transient nature of orbital forcing it could be argued that a suite of 1 kyr simulations using fixed astronomical forcing might be expected to predict less variation than a transient simulation covering the same time interval where orbital forcing was continuously updated in the model. Thus continuing simulations to 1 kyr years without altering orbital forcing could bias our results towards stability. To ensure consistency in our model results that are used in our calculations of maximum SAT variation, we utilise the results from the 500 year simulations in all cases (the impact of this choice is demonstrated in Supplementary Fig. 9).

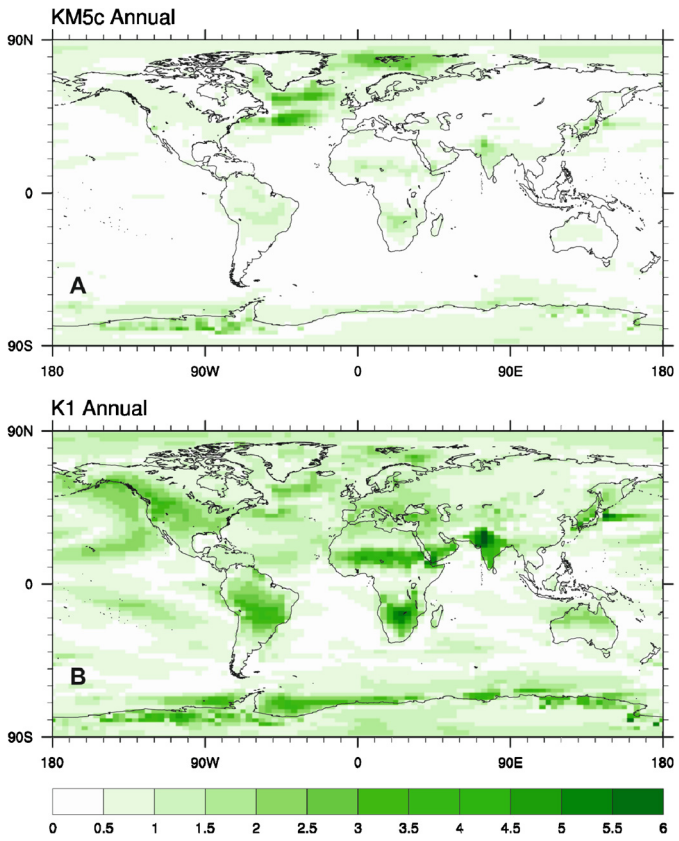

Fig. 5. Maximum annual SAT change (°C) derived from 10 orbital sensitivity simulations differenced from the MIS KM5c (A) and the K1 (B) controls, in each grid square. See text in Section 3.3 for further explanation.

The maximum difference in SAT around the K1 interglacial is in general, much larger than around KM5c (Fig. 5). The changes in terrestrial SATs are also larger reaching 7.7 °C in India. There are also substantial changes over Central and Southern Africa (5.6 °C), North and South America (4 °C) and Antarctica (5.1 °C). Globally there is a 2 °C maximum orbitally induced variation over the oceans.

In K1 there is a similar dipole pattern in the North Atlantic, although less intense, in three simulations are also associated with changes in salinity, sea ice and ocean mixed layer depth. Other differences in the K1 sensitivity experiments such as cooling over Antarctica are associated with increases in sea ice in this region. Large terrestrial SAT changes are effected by orbit and insolation. It is worthwhile noting that the Earth as global annual mean received 0.5 W m^{-2} insolation at the top of the atmosphere compared to present day or the KM5c time slice. This is also demonstrated in Supplementary Fig. 4 showing incoming short wave radiation for the K1 orbital sensitivity experiments. These strong orbitally forced terrestrial changes in SATs shown in 7 of the simulations in Fig. 4, are also linked to increased changes in precipitation, especially in regions of South America, South Africa and Northern Africa. The patterns of SAT change in the orbital sensitivity experiment also indicate a possible shift in the position of the inter-tropical convergence zone in response to the altered equator to pole temperature gradient.

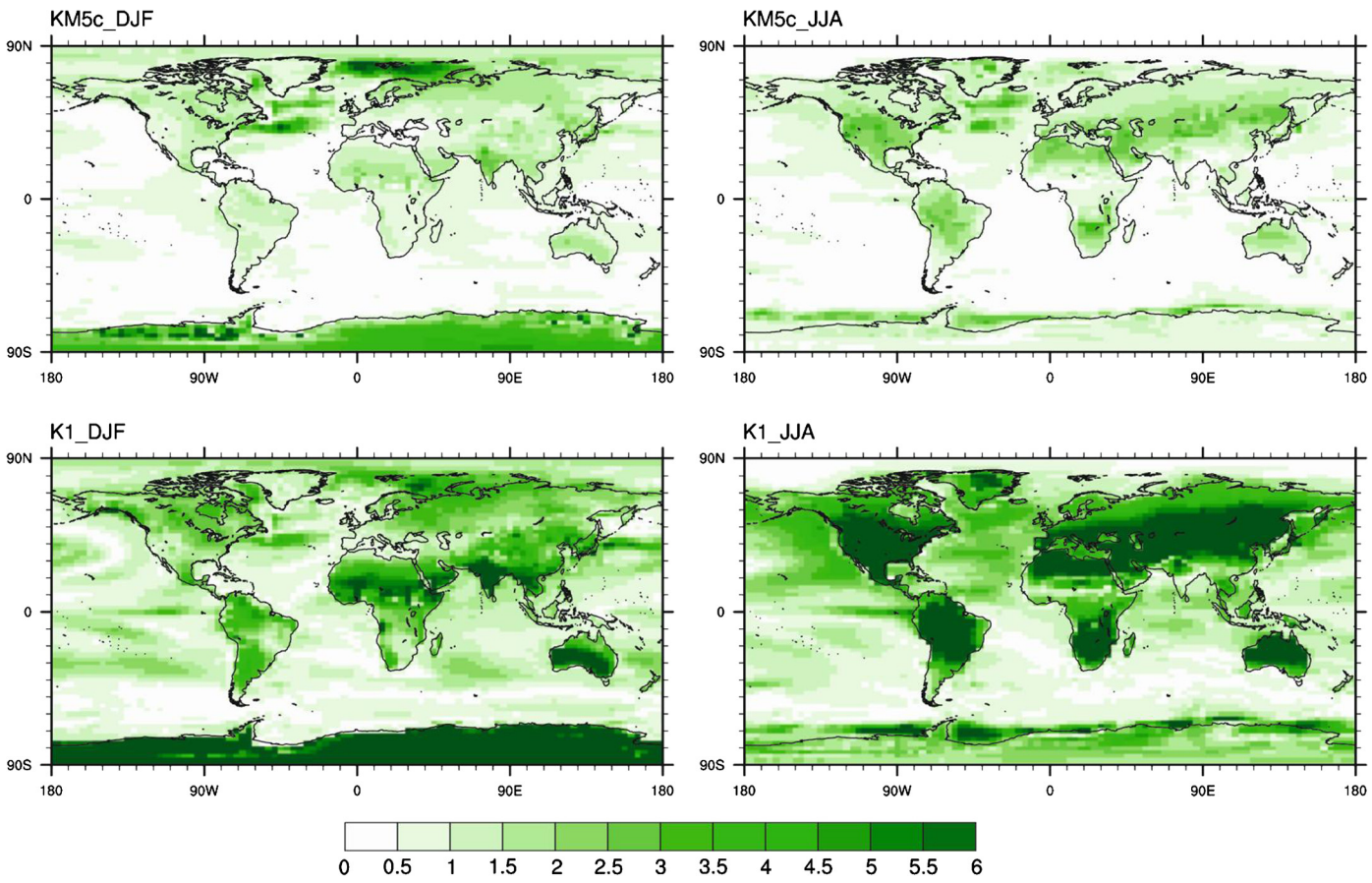

Fig. 6. Maximum seasonal SAT change (°C) derived from 10 orbital sensitivity simulations differenced from the MIS KM5c (left) and the K1 (right) controls, in each grid square. (top left) KM5c_December, January, February (DJF); (top right) KM5c_June, July, August (JJA); (bottom left) K1_DJF; (bottom right) K1_JJA.

3.4. Patterns of maximum spatial variation in seasonal mean SAT (summer and winter)

Using the procedure described in Section 3.3 we are able to determine that the maximum changes in seasonal SAT driven by orbital forcing (Fig. 6) are larger than the annual maximum difference (Fig. 5) for both KM5c and K1. For KM5c, temperature differences reach 6 °C in DJF (December, January, February) in the sea ice regions with JJA (June, July, August) showing larger SAT differences of up to 5 °C over terrestrial areas (South America, South Africa and Australia). The seasonal SAT differences around the K1 interglacial show greater variation than KM5c, reaching 13 °C over Antarctica and 10 °C over India and Australia in DJF, and 12 °C during JJA over the terrestrial areas.

In summary, the maximum annual variation in SAT around K1 (7.9 °C) is shown to be higher than for KM5c (4.8 °C). This is also reflected within the seasonal SAT analysis (Fig. 6), which shows a maximum difference of 21.7 °C in SATs for K1 and 9.3 °C for KM5c. These results are consistent with the changes in insolation at the top of the atmosphere shown in Supplementary Fig. 1.

4. Discussion

4.1. Interglacials in the Pliocene

From Quaternary Science we understand that interglacial events can be diverse in character and such a broad term as 'interglacial' can encompass warm episodes of different duration, stability and climatic characteristics (Schreve and Candy, 2010). For the first time we have explored the nature of discrete interglacial events within the Pliocene epoch. Our analyses have demonstrated that the KM5c and K1 interglacial events are different in nature. Therefore, the results discussed here suggest that treating the mPWP as a single 'average stable interglacial' is not representative of this time as each interglacial is likely to display its own unique characteristics. Additionally, there are an increasing number of proxy records documenting orbital variability in Pliocene surface temperatures (e.g. Lawrence et al., 2006; Dekens et al., 2008; Etourneau et al., 2009; Naafs et al., 2012; Rosell-Melé et al., 2014).

4.2. Implications for data-model comparison

Traditionally, data-model comparison (DMC) studies for the Pliocene have focused on mean annual temperatures for a defined time slab encompassing different orbital forcing (e.g. Dowsett et al., 2012; Salzmann et al., 2013). The differences we have seen in model predictions for KM5c and K1 demonstrate the complications of comparing time averaged proxy data to time specific model simulations. For the purpose of DMC this underlines the importance of new initiatives to reconstruct discrete time slices within the mPWP (Dowsett et al., 2013; Haywood et al., 2013b). KM5c has been identified as a reconstruction target for next phase of the PRISM project (PRISM4: Dowsett et al., 2013). Assuming that it will not be possible to precisely correlate all proxy records to the peak of the KM5c event, our results indicate that as long as proxy data reflect mean annual SAT, then the effect of variations in SAT around the benthic oxygen isotope peak KM5c will have an overall small effect on DMC. For example, in Fig. 5 most areas show maximum SAT deviation from $Plio^{CTL}KM5c^{3205}$ of less than 1 °C. However, the magnitude of SAT change around K1 is larger, dictating the necessity for even higher resolution chronology compared to KM5c, although this may be difficult to achieve.

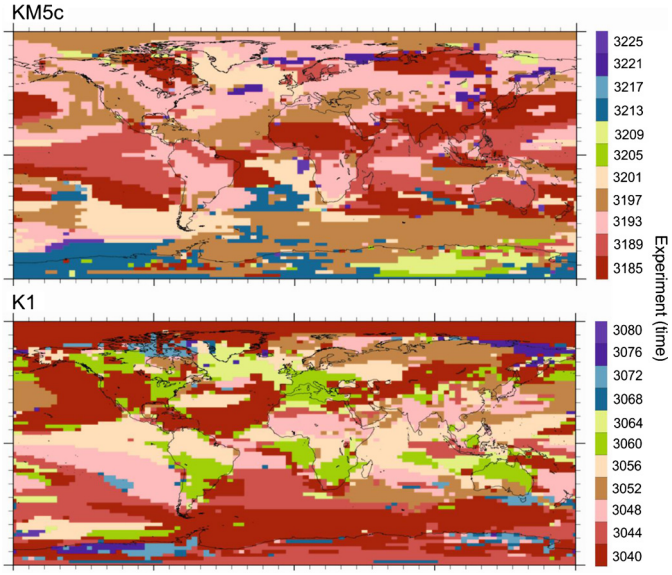

Fig. 7. Maximum SAT around each interglacial peak: colours denote model simulations in which maximum temperature occurred per model grid square. This indicates that maximum temperature for each interglacial was not synchronous and also varied between KM5c and K1.

However, if proxy data represent seasonal temperatures the SAT variation is more significant with regard to DMC, especially at higher latitudes. Fig. 6 shows up to 7 °C of SAT change in the Nordic Seas and Antarctica for DJF and up to 3.5 °C change in most terrestrial areas in JJA for the KM5c interglacial.

4.3. Assessing the synchroneity of peak temperatures

In this study we have assessed the synchroneity of peak warming around two interglacial events. Out results show that peak warmth is not synchronous, instead we see a complex mosaic of responses whereby in specific regions maximum temperature change is largely synchronous, yet in other regions maximum temperature may be diachronous by as much as 40 kyr. This can be seen in Fig. 7 for both KM5c and K1. The diachronous nature of warming demonstrated in our model results implies that aligning or adjusting proxy temperature time series (so that warm/cold peaks always correlate) can result in significant temporal miscorrelation. The end result would be a reconstruction of maximum temperatures at multiple locations that did not coexist in a temporal sense. This has implications for both regional and global synoptic temperature reconstructions, as well as studies investigating dominant drivers of climate.

At this time, the majority of disagreements between Pliocene simulations and proxy estimates of temperature imply that models underestimate the magnitude of change (Sloan et al., 1996; Dowsett et al., 2010; Lunt et al., 2012; Salzmann et al., 2013). If peak warming is diachronous, then this provides a mechanism to at least partly account for this discrepancy. Independent determination of synchroneity in peak temperatures in marine/terrestrial records is difficult to achieve. Thus pre-Quaternary DMC requires a methodology which incorporates the effects of orbital forcing on climate variability and the potential effects of diachronous proxy-based temperature estimates.

4.4. Caveats/future work

In this study we have looked at the effects of orbital forcing. We have not incorporated additional feedbacks associated with changes in orbital forcing (i.e. those associated with ice-sheet evolution and vegetation change). It is therefore possible that our maximum changes in SAT could be under or overestimated. Given the nature of the K1 event and the changes in orbital forcing compared to modern, the assumption of limited feedbacks from ice sheets and vegetation cover around this interglacial is more difficult to justify than KM5c. Future work will look at these two additional feedbacks alongside changing orbit. We have not run simulations in which CO_2 covaried with orbit, but we do know there is a relationship between CO_2 and orbital forcing from the late Pleistocene (Saltzman and Maasch, 1988; Berger et al., 1999). However, most CO_2 reconstructions have relatively low temporal resolution. Therefore, accounting for this in a meaningful way in our experimental design is difficult. New records of atmospheric CO_2 such as Badger et al. (2013) show relatively stable levels of CO_2 using an alkenone carbon isotope-based record at high temporal but more records are needed.

5. Conclusion

In this paper we query the traditional view of the mPWP as having stable climate conditions. Using HadCM3 we present the first suite of orbital sensitivity experiments around the KM5c and K1 interglacial peaks in order to assess the nature of climate variability around two discrete interglacial events within the mPWP. We find that:

- Maximum mean annual temperature variation around the K1 interglacial is higher than around KM5c, and the spatial patterns of these SAT differences vary between the two interglacials.
- In a seasonal analysis, the maximum difference in temperature around the KM5c and K1 interglacials are larger than the mean annual changes.
- The maximum warming shown in the simulations 40 kyr around the interglacial peaks, both spatially and temporally were not consistent between the two interglacial events: this implies that the variation in maximum warming are dependent upon the nature of orbital forcing.

In the context of future climate change, orbital forcing is not a significant factor that will influence climate over politically or socially meaningful timescales. Therefore, for the Pliocene to inform us about the long term effects of near modern CO_2 concentrations, it is necessary to reconstruct an interglacial event(s) in the Pliocene that displays modern/near modern orbital forcing (Haywood et al., 2013b). The results presented here have highlighted diversity in the nature of Pliocene interglacials. While the averaging of these interglacial events (Dowsett and Poore, 1991; Dowsett, 2007) may generally show the same broad patterns of global mean annual SAT change, it will mask significant variations in regional and seasonal temperature change critical to the robust assessment of climate model performance. In order to successfully compare model results and proxy data to form significant conclusions about model fidelity, a time slice rather than a time-averaged approach is needed. The issues discussed here are not only relevant to Pliocene climate, but to any pre-Quaternary interval, and the effects of time averaging and non-synchroneity are likely to be exacerbated further back in time due to weaker chronological constraints on proxy data.

Acknowledgements

C.L.P., A.M.H., A.M.D., S.J.H. and S.J.P. acknowledge that the research leading to these results has received funding from the European Research Council under the European Union's Seventh

Framework Programme (FP7/2007–2013)/ERC grant agreement no. 278636. J.O.P. acknowledges the UK Natural Environment Research Council (NERC) for the provision of a Doctoral Training Grant NE/H5246734/1. The authors would like to thank Harry Dowsett of the US Geological Survey for his insightful contributions to the manuscript.

Appendix A. Supplementary material

Supplementary material related to this article can be found online at http://dx.doi.org/10.1016/j.epsl.2014.05.030.

References

Badger, M.P.S., Schmidt, D.N., Mackensen, A., Pancost, R.D., 2013. High-resolution alkenone palaeobarometry indicates relatively stable pCO_2 during the Pliocene (3.3–2.8 Ma). Philos. Trans. R. Soc. A 371, 20130094. http://dx.doi.org/10.1098/rsta.2013.0094.

Berger, A., Li, X.S., Loutre, M.-F., 1999. Modelling northern hemisphere ice volume over the last 3 Ma. Quat. Sci. Rev. 18, 1–11. http://dx.doi.org/10.1016/S0277-3791(98)00033-X.

Bragg, F., Lunt, D.J., Haywood, A.M., 2012. Mid-Pliocene climate modelled using the UK Hadley Centre Model: PlioMIP Experiments 1 and 2. Geosci. Model Dev. 5, 1109–1125.

Cattle, H., Crossley, J., 1995. Modelling Arctic climate change. Philos. Trans. R. Soc. 352, 201–213.

Chan, W.L., Abe-Ouchi, A., Ohgaito, R., 2011. Simulating the mid-Pliocene climate with the MIROC general circulation model: experimental design and initial results. Geosci. Model Dev. 4, 1035–1049.

Cox, P.M., Betts, R.A., Bunton, C.B., Essery, R.L.H., Rowntree, P.R., Smith, J., 1999. The impact of new land surface physics on the GCM simulation of climate and climate sensitivity. Clim. Dyn. 15, 183–203.

Cronin, T.M., Whatley, R.C., Wood, A., Tsukagoshi, A., Ikeya, N., Brouwers, E.M., Briggs, W.M., 1993. Microfaunal evidence for elevated mid-Pliocene temperatures in the Arctic Ocean. Paleoceanography 8, 161–173.

Cusack, S., Slingo, A., Edwards, J.M., Wild, M., 1998. The radiative impact of a simple aerosol climate on the Hadley Centre atmospheric GCM. Q. J. R. Meteorol. Soc. 124, 2517–2526.

Dekens, P.S., Ravelo, A.C., McCarthy, M.D., 2007. Warm Upwelling Regions in the Pliocene Warm Period. Paleoceanography 22, PA3211. http://dx.doi.org/10.1029/2006PA001394.

Dekens, P.S., Ravelo, A.C., McCarthy, M.D., Edwards, C.A., 2008. A 5 million year comparison of Mg/Ca and alkenone paleo-thermometers. Geochem. Geophys. Geosyst. 9, 1525–2027. http://dx.doi.org/10.1029/2007GC001931.

Dolan, A.M., Haywood, A.M., Hill, D.J., Dowsett, H.J., Hunter, S.J., Lunt, D.J., Pickering, S., 2011. Sensitivity of Pliocene ice sheets to orbital forcing. Palaeogeogr. Palaeoclimatol. Palaeoecol. 309, 98–110.

Dowsett, H.J., 2007. The PRISM palaeoclimate reconstruction and Pliocene sea-surface temperature. In: Williams, M., Haywood, A.M., Gregory, J., Schmidt, D.N. (Eds.), Deep-time Perspectives on Climate Change: Marrying the Signal from Computer Models and Biological Proxies: London, UK. In: Micropalaeontological Society Special Publications. Geological Society of London, pp. 459–480.

Dowsett, H.J., Poore, R.Z., 1991. Pliocene sea surface temperatures of the North Atlantic Ocean at 3.0 Ma. Quat. Sci. Rev. 10, 189–204.

Dowsett, H.J., Robinson, M., Haywood, A.M., Salzmann, U., Hill, D.J., Sohl, L., Chandler, M.A., Williams, M., Foley, K., Stoll, D., 2010. The PRISM3D Paleoenvironmental reconstruction. Stratigraphy 7, 123–139.

Dowsett, H.J., Haywood, A.M., Valdes, P.J., Robinson, M.M., Lunt, D.J., Hill, D.J., Stoll, D.K., Foley, K.M., 2011. Sea surface temperatures of the mid-Piacenzian Warm Period: a comparison of PRISM3 and HadCM3. Palaeogeogr. Palaeoclimatol. Palaeoecol. 309, 83–91.

Dowsett, H.J., Robinson, M.M., Haywood, A.M., Hill, D.J., Dolan, A.M., Stoll, D.K., Chan, W.L., Abe-Ouchi, A., Chandler, M.A., Rosenbloom, N.A., Otto-Bliesner, B.L., Bragg, F.J., Lunt, D.J., Foley, K.M., Riesselman, C.R., 2012. Assessing confidence in Pliocene sea surface temperatures to evaluate predictive models. Nat. Clim. Change. http://dx.doi.org/10.1038/NCLIMATE1455.

Dowsett, H.J., Robinson, M.M., Stoll, D.K., Foley, K.M., Johnson, A.L.A., Williams, M., Riesselman, C.R., 2013. The PRISM (Pliocene palaeoclimate) reconstruction: time for a paradigm shift. Philos. Trans. R. Soc. 371, 20120524.

Edwards, J.M., Slingo, A., 1996. Studies with a flexible new radiation code. I: Choosing a configuration for a large scale model. Q. J. R. Meteorol. Soc. 122, 689–719.

Etourneau, J., Martinez, P., Blanz, T., Schneider, R., 2009. Pliocene–Pleistocene variability of upwelling activity, productivity, and nutrient cycling in the Benguela region. Geology 37, 871–874.

Gent, P.R., McWilliams, J.C., 1990. Isopycnal mixing in ocean circulation models. J. Phys. Oceanogr. 20, 150–155.

Gordon, C., Cooper, C., Senior, C.A., Banks, H., Gregory, J.M., Johns, T.C., Mitchell, J.F.B., Wood, R.A., 2000. The simulation of SST, sea ice extents and ocean heat transports in a version of the Hadley Centre coupled model without flux adjustments. Clim. Dyn. 16, 147–168.

Gradstein, F.M., Ogg, J.G., Smith, A.G., 2004. A Geologic Time Scale 2004. Cambridge University Press, 589 pp.

Gregory, J.M., Mitchell, J.F.B., 1997. The climate response to CO_2 of the Hadley Centre coupled AOGCM with and without flux adjustment. Geophys. Res. Lett. 24, 1943–1946.

Gregory, D., Kershaw, R., Inness, P.M., 1997. Parametrization of momentum transport by convection, 2. Tests in single-column and general circulation models. Q. J. R. Meteorol. Soc. 123, 1153–1183.

Haywood, A.M., Valdes, P.J., 2004. Modelling Middle Pliocene warmth: contribution of atmosphere, oceans and cryosphere. Earth Planet. Sci. Lett. 218, 363–377.

Haywood, A.M., Valdes, P.J., Sellwood, B.W., 2000. Global scale palaeoclimate reconstruction of the middle Pliocene climate using the UKMO GCM: initial results. Glob. Planet. Change 25, 239–256.

Haywood, A.M., Dowsett, H.J., Otto-Bliesner, B., Chandler, M.A., Dolan, A.M., Hill, D.J., Lunt, D.J., Robinson, M.M., Rosenbloom, N., Salzmann, U., Sohl, L.E., 2010. Pliocene Model Intercomparison Project (PlioMIP): experimental design and boundary conditions (Experiment 1). Geosci. Model Dev. 3, 227–242.

Haywood, A.M., Dowsett, H.J., Robinson, M.M., Stoll, D.K., Dolan, A.M., Lunt, D.J., Otto-Bliesner, B., Chandler, M.A., 2011. Pliocene Model Intercomparison Project (PlioMIP): experimental design and boundary conditions (Experiment 2). Geosci. Model Dev. 4, 571–577.

Haywood, A.M., Hill, D.J., Dolan, A.M., Otto-Bliesner, B.L., Bragg, F., Chan, W.-L., Chandler, M.A., Contoux, C., Dowsett, H.J., Jost, A., Kamae, Y., Lohmann, G., Lunt, D.J., Abe-Ouchi, A., Pickering, S.J., Ramstein, G., Rosenbloom, N.A., Salzmann, U., Sohl, L., Stepanek, C., Ueda, H., Yan, Q., Zhang, Z., 2013a. Large-scale features of Pliocene climate: results from the Pliocene Model Intercomparison Project. Clim. Past 20 (2), 103.

Haywood, A.M., Dolan, A.M., Pickering, S.J., Dowsett, H.J., McClymont, E.L., Prescott, C.L., Salzmann, U., Hill, D.J., Hunter, S.J., Lunt, D.J., Pope, J.O., Valdes, P.J., 2013b. On the identification of a Pliocene time slice for data-model comparison. Philos. Trans. R. Soc. 371. http://dx.doi.org/10.1098/rsta.2012.0515. 20120515.

Hill, D.J., Dolan, A.M., Haywood, A.M., Hunter, S.J., Stoll, D.K., 2010. Sensitivity of the Greenland Ice Sheet to Pliocene sea surface temperatures. Stratigraphy 7, 111–122.

Joussaume, S., Braconnot, P., 1997. Sensitivity of paleoclimate simulation results to the season definitions. J. Geophys. Res., Atmos. 102, 1943–1956.

Laskar, J., Robutel, P., Joutel, F., Gastineau, M., Correia, A.C.M., Levrard, B., 2004. A long term numerical solution for the insolation quantities of the Earth. Astron. Astrophys. 428, 261–285.

Lawrence, K.T., Liu, Z., Herbert, T.D., 2006. Evolution of the eastern tropical Pacific through Plio-Pleistocene glaciation. Science 312, 79–83.

Lisiecki, L.E., Raymo, M.E., 2005. A Pliocene–Pleistocene stack of 57 globally distributed benthic delta O-18 records. Paleoceanography 20, PA1003.

Lunt, D.J., Foster, G.L., Haywood, A.M., Stone, E.J., 2008. Late Pliocene Greenland glaciation controlled by a decline in atmospheric CO_2 levels. Nature 454, 1102–1105. http://dx.doi.org/10.1038/nature07223.

Lunt, D.J., Haywood, A.M., Schmidt, G.A., Salzmann, U., Valdes, P.J., Dowsett, D.J., Loptson, C.A., 2012. On the causes of mid-Pliocene warmth and polar amplification. Earth Planet. Sci. Lett. 321–322, 128–138.

Miller, K.G., Wright, J.D., Browning, J.V., Kulpecz, A., Kominz, M., Naish, T.R., Cramer, B.S., Rosenthal, Y., Peltier, R., Sosdian, S., 2012. High tide of the warm Pliocene: implications of global sea level for Antarctic deglaciation. Geology. http://dx.doi.org/10.1130/G32869.1.

Moran, K., et al., 2006. The Cenozoic palaeoenvironment of the Arctic Ocean. Nature 441, 601–605.

Naafs, B.D.A., Hefter, J., Acton, G., Haug, G.H., Martínez-Garcia, A., Pancost, R., Stein, R., 2012. Strengthening of North American dust sources during the late Pliocene (2.7 Ma). Earth Planet. Sci. Lett. 317–318, 8–19. With Research Highlight in: Newton, A., 2012. Dustytransition. Nat. Geosci. 5 (2), 91.

Naish, T., et al., 2009. Obliquity-paced Pliocene West Antarctic ice sheet oscillations. Nature 458, 322–328.

Pollard, D., DeConto, R.M., 2009. Modelling West Antarctic ice sheet growth and collapse through the past five million years. Nature 458, 329–332.

Polyak, L., et al., 2010. History of sea-ice in the Arctic. Quat. Sci. Rev. 29, 1757–1778.

Rosell-Melé, A., Martínez-Garcia, A., McClymont, E.L., 2014. Persistent warmth across the Benguela upwelling system during the Pliocene epoch. Earth Planet. Sci. Lett. 386, 10–20.

Saltzman, B., Maasch, K.A., 1988. Carbon cycle instability as a cause of the Late Pleistocene Ice Age Oscillations: modeling the asymmetric response. Glob. Biogeochem. Cycles 2, 177–185.

Salzmann, U., Haywood, A.M., Lunt, D.J., Valdes, P.J., Hill, D.J., 2008. A new global biome reconstruction and data-model comparison for the Middle Pliocene. Glob. Ecol. Biogeogr. 17, 432–447.

Salzmann, U., Dolan, A.M., Haywood, A.M., Chan, W.-L., Voss, J., Hill, D.J., Abe-Ouchi, A., Otto-Bliesner, B.L., Bragg, F.J., Chandler, M.A., Contoux, C., Dowsett, H.J., Jost,

A., Kamae, Y., Lohmann, G., Lunt, D.J., Pickering, S.J., Pound, M.J., Ramstein, G., Rosenbloom, N.A., Sohl, L.E., Stepanek, C., Ueda, H., Zhang, Z.-S., 2013. Challenges in quantifying Pliocene terrestrial warming revealed by data-model discord. Nature Climate Change 3, 969–974.

Schreve, D., Candy, I., 2010. Interglacial climates: advances in our understanding of warm climate episodes. Prog. Phys. Geogr. 34, 845–856.

Shackleton, N.J., Hall, M.A., 1984. Oxygen and Carbon Isotope stratigraphy of Deep Sea Drilling Project Hole 552A: Plio-Pleistocene glacial history. Initial Reports of the Deep Sea Drilling Project. Govt. Printing Office, Washington, pp. 599–609.

Sloan, L.C., Crowley, T.J., Pollard, D., 1996. Modeling of middle Pliocene climate with the NCAR GENESIS general circulation model. Mar. Micropaleontol. 27, 51–61.

Wan, S., Tian, J., Steinke, S., Li, A., Li, T., 2010. Evolution and variability of the East Asian summer monsoon during the Pliocene: evidence from clay mineral records of the South China Sea. Palaeogeogr. Palaeoclimatol. Palaeoecol. 293, 237–247.